PERGAMON

International Journal of Heat and Mass Transfer 42 (1999) 3057–3070

International Journal of HEAT and MASS TRANSFER

Stochastic modeling of nonisothermal flow during resin transfer molding

S.K. Padmanabhan, R. Pitchumani*

Composites Processing Laboratory, Department of Mechanical Engineering, University of Connecticut, U-139, Storrs, CT 06269-3139, USA

Received 9 October 1998; received in revised form 2 December 1998

Abstract

Resin Transfer Molding (RTM) offers the potential to manufacture reinforced thermosetting composites of complex geometries cost-effectively, and at high throughputs. Strong uncertainties inherent in the process, however, stymie robust production of quality composites via this route. Although a number of numerical models have been developed over the years to describe the process, a thorough and systematic analysis of the parameter uncertainties has been the subject of little attention, and forms the focus of this study. This paper presents a stochastic model to investigate the effects of process and material parameter uncertainties on the nonisothermal filling process during resin transfer molding. The analysis is performed in terms of four dimensionless parameters that concisely represent the process physics, and provide for a generalized applicability of the study over a wide range of processing configurations. Parametric studies are conducted to identify optimum values of the dimensionless quantities that minimize the fill time, while simultaneously minimizing the output parameter variabilities. The results of the study provide valuable insight towards robust manufacture of composite materials.

1. Introduction

Resin Transfer Molding (RTM) is a liquid composite molding technique that is increasingly being used in the commercial manufacture of reinforced thermosetting composites. In the basic isothermal process, a catalyzed resin is injected into a closed mold cavity which has a pre-placed fiber stack, called the *preform*, at room temperature [1]. After the resin has completely permeated the preform, the mold walls are subjected to high temperatures in order to initiate complex cross-linking chemical reactions called *cure*. Cure leads to an increase in the viscosity of the resin, and eventually the resin *gels* to form a structurally hard composite product. In the nonisothermal variants of the RTM process, the resin, the mold walls, and the fiber stack are all maintained at different temperatures, and the temperature field inside the mold changes continuously as the resin flows. Nonisothermal mold filling has the potential to result in shorter processing cycles, since heating the resin leads to a decrease in its viscosity, and hence to faster resin flow. It is to be noted, however, that heating the resin also initiates the cure reactions that might cause gelling before the mold is completely filled. Complex nonlinear interactions among the governing phenomena are thus characteristic of the process.

* Corresponding author: Tel.: +1-860-486-0683; fax: +1-860-486-5088.

E-mail address: pitchu@engr.unconn.edu (R. Pitchumani)

0017-9310/99/$ - see front matter
PII: S0017-9310(98)00377-9

Nomenclature

A	aspect ratio
c_p	specific heat capacity [kJ (kg K)$^{-1}$]
Da	Damköhler number
E	activation energy [cal mol^{-1}]
$\bar{E}$	dimensionless activation energy
H	height of the mold [m]
K	frequency factor [min^{-1}]
k_z	thermal conductivity of the composite along the z-direction [W m K^{-1}]
L	length of the mold [m]
m, n	empirical exponents used in the kinetics equation [Eq. (6)]
N	number of samples used in the stochastic analysis
$\bar{P}$	probability encompassed by each of the strata in the LHS technique
p	pressure [bar]
$\bar{p}$	dimensionless pressure
Pe	Peclet number
p_i	inlet pressure [bar]
p_o	ambient pressure [bar]
R	universal gas constant [cal (mol K)$^{-1}$]
T	temperature [K]
$\bar{t}$	dimensionless time
t_c	characteristic time [min]
t_{fill}	mold fill time [min]
U	empirical constant in the expression for viscosity [Eq. (3)]
u	velocity of the resin [m s^{-1}]
$\bar{u}$	dimensionless resin velocity
u_c	characteristic velocity [m s^{-1}]
x, z	rectilinear coordinates
$\bar{x}$, $\bar{z}$	dimensionless lengths along the x- and z-coordinates
Z	multivariate objective function [Eq. (10)]

Greek symbols

α_{max}	maximum degree of cure at the end of mold fill
H_r	heat of the cure reaction [kJ kg^{-1}]
δ	normalized output variance [Eq. (9)]
η	resin viscosity [cP]
$\bar{\eta}$	dimensionless viscosity of the resin
η_c	reference viscosity [cP]
η_w	resin viscosity based on the wall temperature [cP]
κ_x	preform permeability [m^2]
$\bar{\kappa}_x$	dimensionless x-permeability
λ	empirical constant in the viscosity expression [Eq. (3)]
μ	mean of an input parameter distribution
ϕ	porosity of the preform
θ	dimensionless temperature
θ_{ad}	dimensionless adiabatic reaction temperature
ρ	density of the composite [kg m^{-3}]
ρ_r	density of the resin [kg m^{-3}]
σ	standard deviation of an input parameter distribution
σ/μ	normalized deviation of a distribution, used to characterize process uncertainties
τ	dimensionless fill time, t_{fill}/t_c

Subscripts

c	characteristic values
m	mean values
o	inlet conditions
w	mold wall conditions
x	direction of resin flow
z	direction along mold thickness

The dominant physical phenomena involved in non-isothermal RTM are the fluid mechanics of the resin permeating the preform, the heat transfer, and the cure kinetics of the resin. The dynamics of the resin flow are in turn influenced by its rheological characteristics and the microstructure of the preform. The kinetic properties of the resin determine its cure behavior, and therefore, the mechanical properties of the composite. The dependence of the resin viscosity on the temperature and cure fields inside the mold closely links the flow and thermochemical phenomena in these processes. A thorough understanding of the process phenomena is essential for designing molds, locating and sizing injection ports and vents, choosing injection pressures for complete permeation, selecting the temperature for optimum mold filling, and determining mold fill times. Toward this end, many experimental investigations of resin flow have been reported in literature [2,3], and numerical models have been developed to simulate the flow of the resin through the porous preforms [4–7]. The cure kinetics of resin systems have also been investigated separately, both experimentally and theoretically [8–11]. The theoretical and experimental studies have played an important role in improving process understanding and guiding process design and optimization.

A fundamental gap, however, exists between the simulations and practice, in that whereas practical manufacturing is carried out amidst a cloud of impreciseness in the material and process parameter values, the available theoretical process models are deterministic in the way they treat the process variables. The uncertainties in the parameters arise from sources such as (a) microstructural variations, which lead to imprecise quantification of the permeability and thermal properties of the preform, and therefore, to unpredictable cure and flow rates, (b) variations in the composition of the resin-catalyst mixture, which result in uncertainties in its rheological properties and the cure reaction parameters, (c) inaccuracies associated with the process monitoring and control, (d) materials variabilities from one vendor to another, and from one batch to another, and (e) environmental uncertainties. In the absence of a systematic effort to control them, these parameter uncertainties can cause large variabilities in the product quality and, therefore, hinder effective process design and control.

It is clear, then, that a systematic analysis of the interactive effects of the process uncertainties on the product quality is imperative for a reliable description of the fabrication process. Furthermore, such an analysis is vital to a robust manufacturing endeavor, which seeks to identify operating regimes that minimize the process output variabilities. Experimental methods such as the Taguchi's factorial design technique [12] provide for statistical process analysis and quality control, and have been used in practical manufacturing applications. However, such methodologies require conducting several processing runs, and as a result, are generally tedious and expensive. Moreover, the resulting process designs are limited to the range of parameter values chosen for the experiments, which may not encompass the true optima.

In this paper, a *stochastic analysis* capability embedded in a simulation framework is presented as an alternative paradigm for analysis and robust design of the process in the face of realistic parameter uncertainties. The uncertain input parameters of a stochastic model are assumed to be random variables that are characterized by probability distributions, and multiple deterministic simulations are performed using appropriately chosen combinations of the input parameters. Stochastic analysis has previously been used in the fields of hydrology and petrology [13], and in safety assessment of technological systems [14–16]. Earlier work by the authors presented the use of stochastic analysis in studying the effects of parameter uncertainties on isothermal mold filling [17] and the cure kinetics of resin systems [18]. The focus of the present investigation is on the nonisothermal mold filling step during resin transfer molding, with the specific goal of studying the variabilities in the mold fill time and resin cure state at the end of mold filling, caused by the input parameter uncertainties.

In this study, a deterministic process model is developed to simulate the coupled flow and cure of the resin during nonisothermal, one-dimensional mold filling. Uncertainties in the preform permeability, the resin viscosity and the kinetic parameters are quantified by assigning appropriate probability distributions to them, and samples are chosen from these distri-

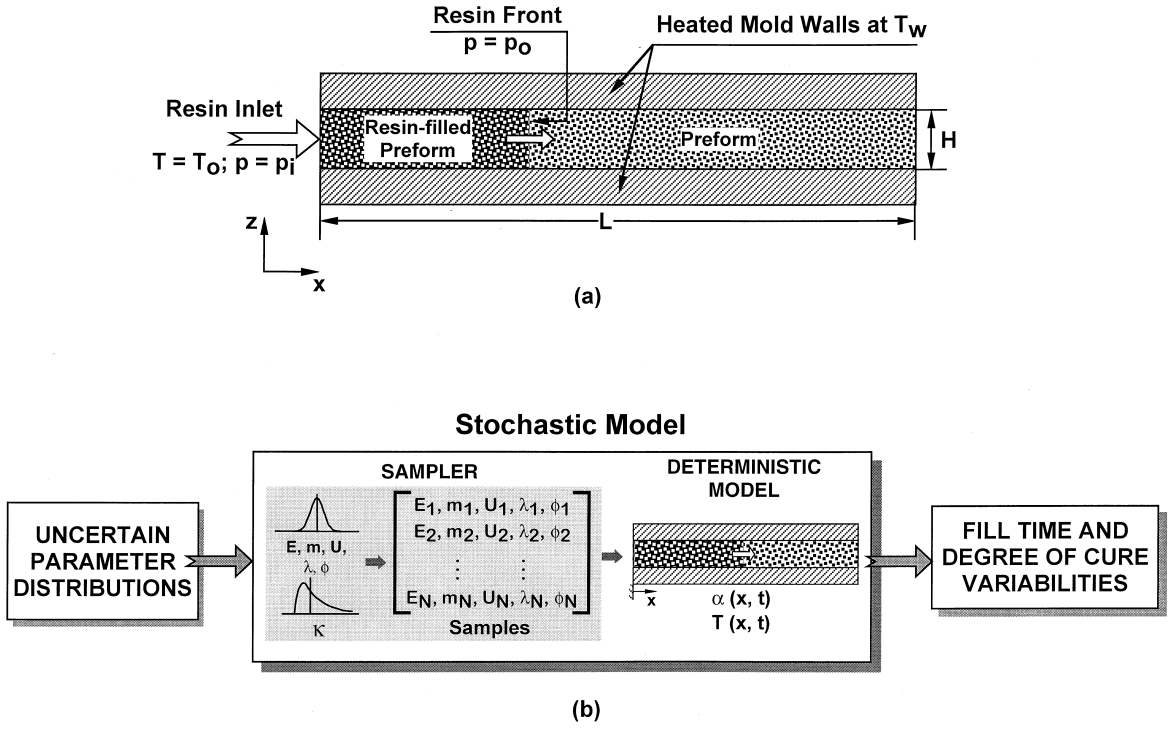

Fig. 1. (a) Schematic of a nonisothermal resin transfer molding process; (b) description of the stochastic modeling methodology.

butions using the Latin Hypercube Sampling (LHS) procedure [19]. The outputs of the stochastic model are probability distributions the fill time, and the maximum cure inside the composite at the end of the filling process. Dimensionless groups that reflect the relative importance of competing physical effects are used to study the output variabilities as a function of the input uncertainties. Optimum values of the dimensionless groups that minimize the fill times while simultaneously reducing output variabilities are identified, and their significance is discussed. The dimensionless groups combine material and process parameters, and consequently provide for a generalized process analysis and optimization.

The deterministic model for the simulation of the mold filling is presented first, and is followed by the development of a stochastic analysis methodology. The results of the study are discussed in Section 4.

2. Deterministic simulation model

Fig. 1(a) shows a schematic of a nonisothermal resin transfer molding process considered in this study. As illustrated in the figure, resin at room temperature (T_o) enters a fibrous preform placed inside a rectangular mold of length L and cavity thickness H. The upper and lower walls of the mold are maintained at an elevated temperature, T_w, throughout the injection process. The resin advances through the preform at a rate determined by the injection pressure, the permeability of the preform, and the viscosity of the resin. Heat transfer from the mold walls accompanies the flow of the resin, and initiates cure reactions inside the resin as a function of the local temperature and the kinetic properties of the resin. The evolution of heat due to the exothermic chemical reaction alters the temperature distribution in the mold, and the transient temperature and the cure fields, in turn, affect the viscosity of the resin, and the rate of mold fill. It is evident, therefore, that nonisothermal mold filling is a complex physical process that involves a number of closely coupled physical phenomena.

Simulation of the combined processes of resin flow, heat transfer, and kinetics of the cure reaction requires a simultaneous solution of the partial differential equations governing these physical phenomena. A detailed analysis of the RTM process needs to consider three-dimensional flow of the resin, along with the accompanying thermochemical phenomena, as presented in the literature [1,7]. However, since the principal focus of this study is to present a methodology for a systematic analysis of the effects of the various parameter uncertainties on the process variabilities, a one-dimensional flow and thermochemical model is used in this investigation.

The one-dimensional resin advancement through the preform is modeled as flow through a porous medium. The effects of the heated mold walls on filling are included by considering the instantaneous viscosity of the resin to be a function of the local temperature and degree of cure. The temperature profiles inside the mold are determined by solving the two-dimensional energy equation in the x- and z-directions. An Arrhenius type empirical equation is used to describe the cure kinetics and to calculate the degree of cure distribution in the composite. All the equations are presented below in their dimensionless forms.

The flow of the resin through the porous preform can be described using Darcy's law, which for a Cartesian x–y coordinate system, is written as follows:

$$\bar{u} = -\frac{\bar{\kappa}_x}{\bar{\eta}}\left(\frac{\mathrm{d}\bar{p}}{\mathrm{d}\bar{x}}\right) \tag{1}$$

where $\bar{\kappa}_x$ is a dimensionless permeability of the porous medium in the direction of flow, $\bar{p}$ is the dimensionless pressure inside the flow domain, $\bar{\eta}$ is the nondimensional viscosity of the resin, and $\bar{u}$ is the normalized velocity in the x-direction. The dimensionless parameters in Eq. (1) are defined as follows:

$$\bar{u} = \frac{u}{u_c}; \quad \bar{p} = \frac{p - p_o}{p_i - p_o}; \quad \bar{\kappa}_x = \frac{\kappa_x}{\kappa_{xm}}; \quad \bar{x} = \frac{x}{H}; \quad \bar{\eta} = \frac{\eta}{\eta_w} \tag{2}$$

where p_i in the inlet resin, p_o is the ambient pressure,

$$u_c = \frac{\kappa_{xm}}{\eta_w}\frac{p_i - p_o}{L}$$

is a characteristic velocity of flow, κ_{xm} is the mean permeability of the preform in the flow direction that may be evaluated using a theoretical model such as [20], H is the thickness of the mold cavity, and η_w is a characteristic viscosity, evaluated at the temperature of the mold walls, T_w, and corresponding to zero degree of cure. The viscosity of the resin at any location inside the mold, η, is expressed as an exponential function of the local temperature and cure [1], as follows:

$$\eta = \eta_c e^{U/RT} e^{\lambda\alpha} \tag{3}$$

where η_c is a reference viscosity used in the rheological characterization, λ and U are empirical constants, R is the universal gas constant, T is the resin temperature in K, and α is the degree of cure, defined as the fraction of the initial resin concentration that has reacted.

In order to determine the velocity of the resin front progression using Eq. (1), the pressure gradients at the flow front need to be evaluated numerically. The pressure field in the resin-filled region of the preform is obtained by substituting for the velocity u in the continuity equation for one-dimensional incompressible flow, to get

$$\frac{\mathrm{d}}{\mathrm{d}\bar{x}}\left(\frac{\bar{\kappa}_x}{\bar{\eta}}\frac{\mathrm{d}\bar{p}}{\mathrm{d}\bar{x}}\right) = 0 \tag{4}$$

The boundary conditions for resin flow are presented in Fig. 1(a), and are stated as follows: At the inlet, the pressure is constant, and is equal to the injection pressure, i.e., $\bar{p} = 1$. At the resin front, the pressure is equal to the ambient pressure, i.e., $\bar{p} = 0$.

The pressure field in the resin-saturated preform region (the dark-shaded region in Fig. 1(a)), and hence the rates of resin permeation, are closely linked to the temperature and cure distribution inside the mold, through the resin viscosity (Eq. (3)). The temperature and cure profiles in the preform are obtained as solutions of the coupled energy and reaction kinetics equations. The two-dimensional energy equation, describing heat conduction through the thickness of the composite (z-direction in Fig. 1(a)) and advection along the direction of flow (x-direction in Fig. 1(a)), may be written as follows in its dimensionless form:

$$\frac{\partial\theta}{\partial\bar{t}} + \left(\bar{u}\cdot\frac{A\phi}{\overline{\rho c_p}}\right)\frac{\partial\theta}{\partial\bar{x}} = \frac{A^2}{Pe}\cdot\frac{\partial^2\theta}{\partial\bar{z}^2} + \phi\cdot\theta_{ad}\cdot Da\cdot e^{-\frac{\bar{E}}{\theta}}\alpha^m(1-\alpha)^n \tag{5}$$

while the reaction kinetics accounting for mass advection is described by the cure equation:

$$\frac{\mathrm{d}\alpha}{\mathrm{d}\bar{t}} + A\cdot\bar{u}\cdot\frac{\mathrm{d}\alpha}{\mathrm{d}\bar{x}} = Da\cdot e^{-\frac{\bar{E}}{\theta}}\alpha^m(1-\alpha)^n \tag{6}$$

where θ is the dimensionless temperature, $\bar{t}$ is the normalized time, ϕ is the porosity of the preform, α is the degree of cure, and $\overline{\rho c_p}$ is an average composite heat capacity. The last term of the energy equation, Eq. (5), represents the rate of evolution of heat due to the exothermic cure reaction, in which the cure rate is described by an empirical Arrhenius-type equation. The empirical constants m and n appearing in Eqs. (5) and (6) are related by the equation $m + n = 2$, as is typically observed for autocatalytic reactions [9]. Furthermore, the term A denotes the aspect ratio (L/H) of the mold cavity.

In both Eqs. (5) and (6), all the spatial variables are normalized with respect to the thickness, H of the mold, and the temperature and time are nondimensionalized with respect to the mold wall temperature and a characteristic fill time, respectively, as follows:

$$\theta = \frac{T}{T_w}; \quad \bar{t} = \frac{t}{t_c}; \quad t_c = \frac{L}{u_c}$$

A number of nondimensional parameters arise when the physical equations describing heat transfer and cure are written in their dimensionless forms, as in Eqs. (5) and (6). The principal nondimensional quantities, namely the Peclet number, Pe, the dimensionless activation energy, $\bar{E}$, the adiabatic reaction temperature, θ_{ad}, and the Damköhler number, Da, are defined as follows:

$$Pe = \frac{u_c \cdot L}{\left(\frac{k_z}{\bar{\rho}\,\bar{c}_p}\right)}; \quad \bar{E} = \frac{E}{RT_w}; \quad \theta_{ad} = \frac{\rho_r \cdot H_r}{T_w \cdot (\overline{\rho c_p})}; \qquad (7)$$

$$Da = K \cdot t_c$$

where k_z is the composite thermal conductivity in the z-direction, ρ_r is the resin density, H_r is the heat of the exothermic cure reaction, E is the activation energy for the reaction, and K is the frequency factor.

The normalized boundary conditions for the energy Eq. (5), can be stated as follows: the top and the bottom surfaces of the mold are maintained at constant temperature, i.e., at $\bar{z} = 0$ and $\bar{z} = 1$, $\theta = 1$. At the beginning of fill, the preform is at ambient temperature, i.e., $\theta(\bar{t} = 0) = \theta_0$, while the mold walls are heated. Similarly, the kinetics Eq. (6), is associated with the condition that the mold inlet, the resin is uncured, i.e., at $\bar{x} = 0$, $\alpha = 0$.

The numerical simulation of the process consists of solving Eqs. (4–6) simultaneously to determine successive locations of the resin flow front as a function of time. The temperature and cure fields in the resin filled region are determined by using an ADI scheme [21] to solve the coupled thermochemical Eqs. (5) and (6). The resin viscosity, which is required for determining the pressure distribution, is calculated as a function of the temperature and cure using Eq. (3), and averaged over the thickness of the composite. The complex spatial dependence of the viscosity necessitates a numerical solution of Eq. (4) for the pressure field. Darcy's law (Eq. (1)) is used to calculate the resin front velocities from the computed pressure distribution, and the flow front is advanced to its next location inside the mold. The above sequence is repeated until the resin fills the mold completely.

The deterministic simulation model described above forms the basis of the stochastic framework detailed in the next section.

3. Stochastic modeling

Stochastic modeling is a method for systematic investigation of process uncertainties, and is based on the simulation of associated physical phenomena for special, but randomly selected stochastic instances [22]. The variabilities in the process are evaluated by performing repeated deterministic simulations for a number of possible combinations of the uncertain inputs. Fig. 1(b) gives a schematic modeling process, describing the various steps involved, which are explained below.

The three main steps in a stochastic modeling are the quantification of the input parameter uncertainties, the propagation of these uncertainties through a deterministic process model, and evaluation of the resulting output variabilities. The uncertain input parameters of a stochastic model are assumed to be random variables that are described by probability distributions. Different distributions such as normal, log-normal, triangular, and uniform distributions can be used to characterize the input parameter uncertainties. An appropriate sampling technique is used to choose combinations of parameter values from the prescribed input distributions. The capability of the sampling technique to accurately reflect the properties of the input parameter distributions depends greatly on the type of sampling technique, and the number of samples chosen. The effects of the input parameter uncertainties on the output variabilities are assessed using the deterministic model to obtain the output parameter values corresponding to *each* of the sampled input parameter sets. Probability distributions for the output parameters are then generated from the simulation results. The deterministic model thus forms the basis for the stochastic framework, as illustrated in Fig. 1(b).

Identifying the critical uncertain input variables is crucial for a rapid and accurate stochastic analysis. In the specific context of the nonisothermal mold filling process under present consideration, the principal sources of process variabilities are the preform microstructure, and the uncertainties associated with the rheological and kinetic characterization of the resin. In particular, the permeability (κ_x), the preform porosity, ϕ (which in turn influences the permeability and properties such as the composite thermal conductivity), the rheological parameters (η_c, U, and λ), and the cure kinetics parameters (E, K, and m) exhibit varying levels of uncertainties. Of all these uncertain quantities, however, the preform microstructure forms the single largest source of process variations. Further, owing to their nonlinear influence on the reaction rate (Eqs. (5) and (6)), the activation energy, E, and the empirical parameter, m, are more critical stochastic variables than the frequency factor, K, even for comparable magnitudes of uncertainties on these three parameters [18]. Similarly, the parameters U and λ have a greater effect on the resin viscosity than the reference value η_c (Eq. (3)). Therefore, only six parameters, namely the

preform microstructure parameters (κ_x, ϕ), the kinetic parameters (E, m), and the viscosity parameters (U, λ) were considered to be uncertain. All the input distributions are specified in terms of their respective mean values, μ, and standard deviations, σ. Equivalently, the input uncertainties are quantified in terms of their normalized standard deviation, σ/μ, and the mean, μ.

In order to perform the stochastic analysis, the input distributions need to be sampled to generate combinations of input parameter values. Sampling techniques used for this purpose work by generating a suitable number of samples from the input parameter distributions, so as to reflect the properties of the parent distribution to a desired degree of accuracy. Since stochastic modeling techniques require the invocation of a deterministic model for each input parameter set, the total computational time is a strong function of the number of samples chosen. The sampling technique should, therefore, require the least number of samples in order to represent the parent probability distribution accurately.

Different techniques, such as Monte Carlo sampling [23] and Latin Hypercube Sampling (LHS) [19], are available for sampling from distributions. The Monte Carlo technique chooses samples purely randomly from the range of input parameter values, while LHS is a stratified sampling method which works by dividing the input parameter range into as many intervals of equal probability, $\bar{P}$, as the number of samples, N, such that $N\bar{P}=1$. One value is chosen from each interval, and the values generated for all the input parameters are combined randomly to form N input parameter sets. Note that a stratified sampling, by virtue of the selection of samples from equiprobable strata spanning the entire distribution, provides a better representation of the distribution, and as a result, requires fewer samples in comparison to purely random sampling using the Monte Carlo technique [24]. The LHS technique is, therefore, used in this analysis to sample the input distributions.

Corresponding to all the input parameter combinations generated by LHS, the deterministic fill time, τ, and the maximum cure of the resin at the end of fill, $\alpha_{\max}$, are calculated using the deterministic numerical model. The calculated process output values are, in turn, used to determine the mean value and variance of the output distributions. The variabilities on the output parameters are quantified by their normalized deviations, defined as follows:

$$\left(\frac{\sigma}{\mu}\right)_{\tau}=\frac{1}{\mu_{\tau}}\sqrt{\sum_{j=1}^{N}\frac{(\tau_j-\mu_{\tau})^2}{N-1}}$$

$$\left(\frac{\sigma}{\mu}\right)_{\alpha_{\max}}=\frac{1}{\mu_{\alpha_{\max}}}\sqrt{\sum_{j=1}^{N}\frac{(\alpha_{\max,\,j}-\mu_{\alpha_{\max}})^2}{N-1}} \tag{8}$$

where μ and σ/μ are, respectively, the mean value and the normalized standard deviation of the output distribution, and the subscripts τ and $\alpha_{\max}$ correspond to the fill time and the maximum cure when the preform is completely permeated. The cumulative magnitude of the output variabilities is quantified using a normalized output variance, δ, defined as

$$\delta=\left[\left(\frac{\sigma}{\mu}\right)_{\tau}^2+\left(\frac{\sigma}{\mu}\right)_{\alpha_{\max}}^2\right] \tag{9}$$

and is used in the presentation of the results of the study.

4. Results and discussion

The stochastic analysis framework described above was used to investigate the effects of the process parameter uncertainties on the nonisothermal mold filling step during resin transfer molding process. The principal goals of the stochastic analysis were the following: (1) to analyze the effects of various dimensionless groups on flow and cure parameter variabilities, and (2) to identify optimal settings for the dimensionless parameters that minimize the fill time and the output variabilities.

The six process and material parameters (κ_x, ϕ, E, m, U and λ) considered in the study were treated as random input variables, and the magnitude of their uncertainties were specified by a 1% normalized standard deviation, i.e., $\sigma/\mu=0.01$. This signifies that the input variables fall within the range defined by $0.97\mu-1.03\mu$ (the $\pm3\sigma$ limits) with 99.7% probability, where μ is the mean value of the input parameter. Five of the uncertain inputs namely the porosity, ϕ, the kinetic parameters (E, m), and the viscosity parameters (U, λ) were described by normal distributions, while the preform permeability, κ_x, was assumed to follow a log-normal distribution, owing to its small magnitude. Table 1 lists the distributions considered for the different input parameters.

As mentioned previously, the Latin Hypercube technique was used to sample from the input distributions. While a sufficiently large number of samples is required for the parameter distributions to be represented accurately, increasing the number of samples also increases the computational time. The minimum sample size required was determined by conducting stochastic simulations for varying number of samples, and examining the output variabilities for convergence. The required sample size was found to depend on the

Table 1
Probability distributions of the uncertain inputs

Parameter	Distribution
Permeability, κ_x	Lognormal
Porosity, ϕ	Normal
Activation energy, E	Normal
Rate exponent, m	Normal
Viscosity parameter, U	Normal
Viscosity exponent, λ	Normal

resin reactivity, and ranged from 1000 for the less-reactive systems to 4000 for resin reactivities at the higher end.

The stochastic simulations were conducted in terms of four different dimensionless quantities, namely, the Peclet number, Pe, the Damköhler number, Da, the dimensionless activation energy, $\bar{E}$, and the adiabatic reaction temperature, θ_{ad}. Physically, the Peclet number is a measure of the relative importance of advection in the direction of resin flow and conduction through the thickness of the composite. A large Peclet number signifies the dominance of advection, while a small Peclet number represents the case where conduction through the thickness dominates the heat transfer. The Damköhler number is the ratio of the fill time scale to the reaction time scale, and signifies how fast the reaction takes place relative to the filling of the mold. The dimensionless activation energy along with the Damköhler number determines the cure rate. The adiabatic reaction temperature denotes the temperature increase potential due to the heat of the reaction, H_r. The dimensional parameters present a concise description of a wide range of material and process parameters, and are used as the basis for a generalized representation of the stochastic simulation results.

The parametric studies were carried out for a wide range of Peclet numbers and different values of the dimensionless activation energy, $\bar{E}$, the Damköhler number, Da, and the adiabatic reaction temperature, θ_{ad}. The range of values considered for the dimensionless groups are listed in Table 2, and are based on the mean values of the stochastic parameters involved. The mean fill time, τ, and the mean value of the maximum cure achieved at the completion of fill, α_{max}, were two of the output parameters of interest. A normalized output variance, δ (Eq. (9)), was used to quantify the cumulative process output variability due to the variances in these two output parameters. The output variance is, in effect, an indicator of the noise to signal ratio of the process, and needs to be minimized in order to achieve robust processing conditions. Thus, one of the objectives of this investigation was to determine the mean values of the dimensionless groups (representing the process and material parameters) that minimize the output variance, δ.

Besides minimizing the process output variabilities, δ, it is additionally desirable to minimize the mean fill time, τ, and achieve as much cure, α_{max}, in the resin as possible at the end of the filling process. Furthermore, it is imperative that the resin fill the mold completely without gelling (onset of crosslinking) prematurely. This constraint may be translated to the mold fill fraction, f, which denotes the fraction of cases for which complete mold filling is achieved, being equal to unity. These competing process requirements can be concisely represented by an objective function, Z, defined as follows:

$$Z = \frac{\tau \cdot \delta}{(1 + \alpha_{max})f} \tag{10}$$

A second goal of the stochastic analysis was, therefore, to determine the processing conditions that minimize the objective function, Z.

Prior to examining the effects of the dimensionless parameters on the process variabilities, it is instructive to understand the combined effects of the thermal and kinetic phenomena on the resin viscosity, which influences the flow of the resin. Fig. 2 shows a typical variation of the resin viscosity with time during an isothermal mold fill. Initially, the degree of cure is generally not sufficient to have an appreciable effect on the viscosity. The initial portion of the curve, therefore, corresponds to the resin viscosity decreasing as a result of the increased temperature (per Eq. (3)) due to the heat transferred from the mold walls. As the residence time available for the crosslinking reaction increases, however, the degree of cure of the resin also increases, and acts in opposition to the temperature

Table 2
Ranges of values of the dimensionless groups in the parametric studies

Dimensionless group	Range
Peclet number, Pe	10^{-2}–10^{9}
Dimensionless activation energy, $\bar{E}$	86.2–94.0
Damköhler number, Da	8×10^{20}–8×10^{23}
Dimensionless adiabatic reaction temperature, θ_{ad}	0.5–10.0

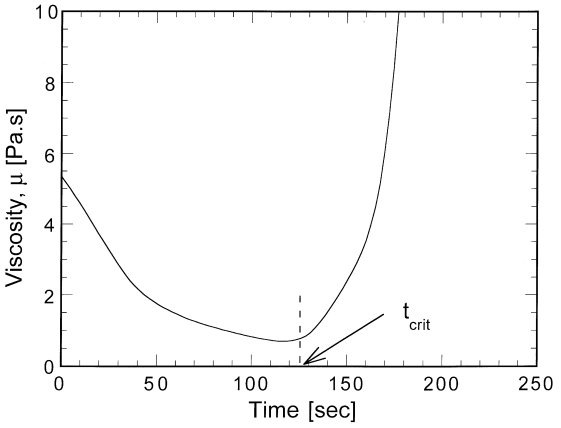

Fig. 2. An example variation of the resin viscosity during isothermal mold filling.

(Eq. (3)) in influencing the viscosity of the resin. After a certain time, t_{crit}, the resin kinetics constitute the dominant viscosity-controlling process, and lead to an increase in the resin viscosity. It is evident that the effects of the degree of cure on resin viscosity lag those of the temperature. The effects of the dimensionless parameters on the interactions between the input process variabilities can be understood better in the light of the results of Fig. 2.

The mean values of the dimensionless fill time, τ, and the maximum degree of cure at the end of mold fill, α_{max}, are plotted in Fig. 3(a, b) as a function of the Peclet number, *Pe*, for four different values of the dimensionless activation energy, $\bar{E}$. It may be seen in Fig. 3(a) that the fill time increases with the Peclet number, which represents a ratio of the conduction time scale to the flow time scale. A smaller value of the Peclet number, therefore, corresponds to the conduction time scale being small, and the increased resin temperature resulting from the rapid heat conduction leads to reduced resin viscosity, and in turn, shorter fill times. Fig. 3(b) shows that for a given activation energy, the maximum degree of cure at the end of mold fill increases with the Peclet number owing to the

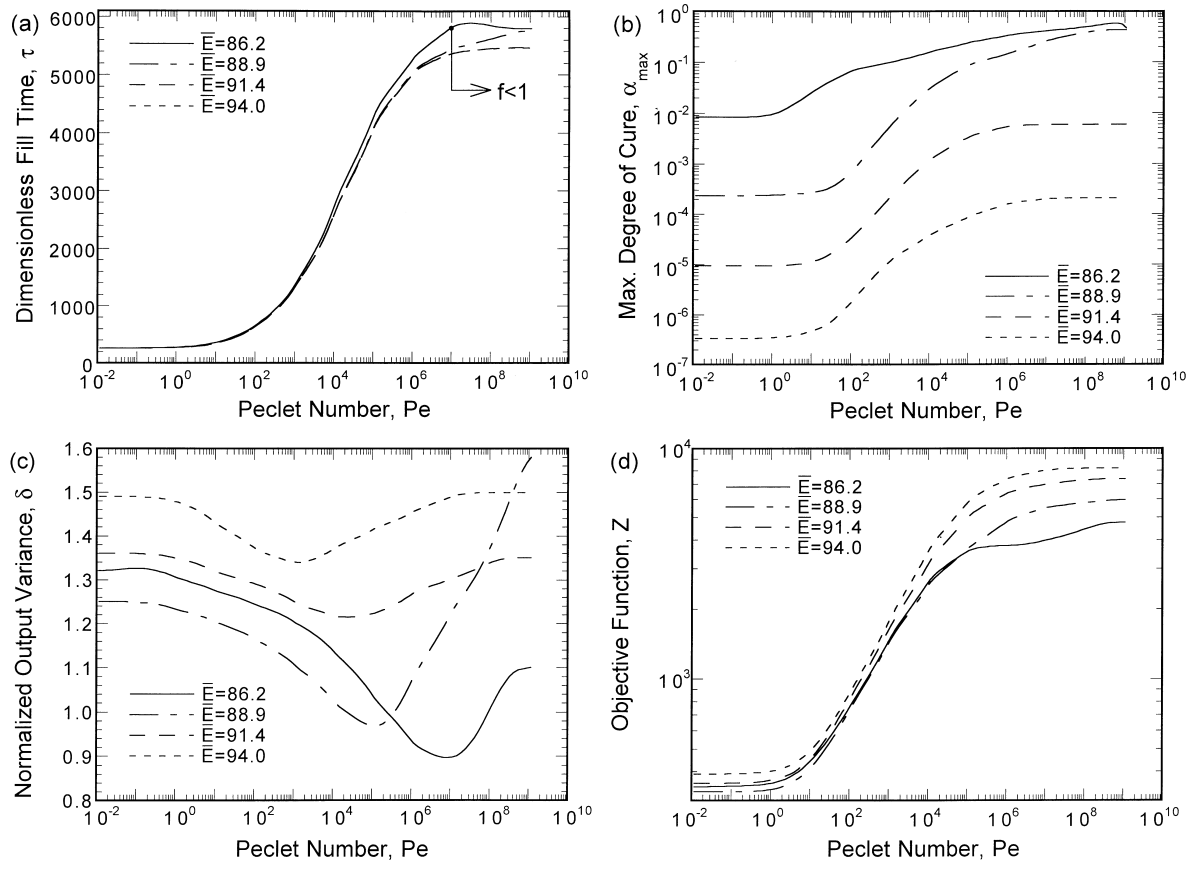

Fig. 3. Variation of the (a) dimensionless fill time, τ, (b) maximum cure at the end of fill, α_{max}, (c) normalized output variance, δ, and (d) multivariate objective function, Z, with Peclet number and the dimensionless activation energy, for $Da = 8 \times 10^{20}$, and $\theta_{ad} = 1.0$.

longer residence time available for the cross-linking reactions. Furthermore, the maximum degree of cure increases with increasing resin reactivity, as denoted by the decreasing activation energy values in Fig. 3(b). In particular, for the smaller activation energies of 86.2 and 88.9, and for intermediate and large Peclet numbers, the degree of cure values are sufficiently high to increase the resin viscosity (corresponding to the trend in the viscosity curve above t_{crit} in Fig. 2). This is reflected in an increase in the fill time for the smaller activation energies, in Fig. 3(a).

It is of interest to note in Fig. 3(b) that for the smallest activation energy studied, over the range of Peclet numbers between about 10^7 and 10^9, the resin gels (i.e., the fractional degree of cure exceeds about 0.5) during the injection process, resulting in an incomplete mold fill. The mean fill time, which is based on the samples that yield complete mold fill only, is therefore seen to decrease over this range of Peclet numbers in Fig. 3(a). It is also evident from Fig. 3(a) that the fill time asymptotically approaches constant high and low values for $Pe \to \infty$ and $Pe \to 0$, respectively. The limit of the Peclet number tending to infinity implies a practically zero conduction inside the preform, and the fill time corresponds to an isothermal fill with the resin being at its inlet temperature. Conversely, very small Peclet numbers correspond to a relatively large conduction inside the composite, which leads to an instantaneous equilibrium of the preform and resin temperature at that of the wall temperature, T_w. The fill time, therefore, corresponds to the low resin viscosity at the high mold wall temperature.

The normalized output variance, δ, defined by Eq. (8), is plotted as a function of the Peclet number and the dimensionless activation energy in Fig. 3(c). It is evident from the results in this plot that for each dimensionless activation energy, there exists a Peclet number that minimizes the output variabilities. Furthermore, the optimum Peclet number shifts towards higher values as the reactivity of the resin increases. The optimum may be interpreted in terms of a window on the reaction rate which minimizes the variabilities. The Arrhenius nature of the cure reaction suggests that resin systems with smaller reactivity, i.e., a large $\bar{E}$, require a higher temperature to achieve a given reaction rate, in comparison with the faster reacting systems. Since the conduction time scale increases with the Peclet number, it follows that the optimum Peclet number increases with decreasing $\bar{E}$ so as to keep the reaction rate within an optimum range. Based on the foregoing reasoning, it may be argued further that for a fixed Peclet number, the output variance will be minimized for a particular value of the dimensionless activation energy, $\bar{E}$. Fig. 3(c) confirms this physical expectation, wherein the optimum values of $\bar{E}$ are seen to be 88.9 for $Pe < 5 \times 10^5$ and 86.2 for $Pe > 5 \times 10^5$, over the scope of the parametric studies conducted. Overall, $\bar{E} = 86.2$ and Peclet numbers in the range 10^6–10^8 are found to result in least output variance during the processing.

Fig. 3(d) shows the variation of the objective function, Z (Eq. (10)), with the Peclet number for different values of the dimensionless activation energy. A comparison of this figure with Fig. 3(a) shows that the objective function is predominantly influenced by the fill time. Although no distinct minima are observed with respect to the Peclet number, resin systems with a higher reactivity ($\bar{E} = 86.2$ and $\bar{E} = 88.9$) are seen to yield lower objective function values over the range of parameters studied.

The effects of the Damköhler number on the process parameters and their variabilities are described in Fig. 4(a–d). Fig. 4(a, b) depicts, respectively, plots of the mean values of the dimensionless fill time, τ, and the maximum degree of cure at the end of mold fill, α_{max}, as a function of the Peclet number, Pe, for four different Damköhler numbers in the range $Da = 8 \times 10^{20}$–8×10^{23}, which represents a spectrum of resin reactivities. Since a large Damköhler number (Da) value represents a highly reactive system, as does a small dimensionless activation energy ($\bar{E}$), the physical trends with respect to increasing values of the Damköhler number are expected to follow those associated with decreasing dimensionless activation energies. A comparison of the results presented in Fig. 4(a, b) vis-à-vis those in Fig. 3(a, b), respectively, reveals this similarity. It is seen in Fig. 4(a) that while the fill time is not significantly influenced by the resin reactivity, i.e., the Damköhler number, at low Peclet numbers, the fill time increases with Damköhler number for large values of the Peclet umber. This behavior may be explained based on the relative magnitudes of the time scales for conduction and reaction, and their resulting influence on the resin cure and viscosity—and in turn, the fill time—as described previously in connection with Fig. 3(a). Furthermore, for a fixed Damköhler number, the fill time and the maximum degree of cure increase with the Peclet number (Fig. 4(a, b)) following a similar variation in Fig. 3(a, b) for a constant dimensionless activation energy. Fig. 4(b) also shows that the degree of cure values for the highest Damköhler number studied (8×10^{23}) are close to the gel point for several cases in the high Peclet number regime, which is reflected in the relatively longer mold fill time values in Fig. 4(a).

The normalized variance on the fill time and the maximum degree of cure at the end of mold fill, δ (Eq. (9)), is plotted as a function of the Peclet number in Fig. 4(c), for the different Damköhler numbers investigated. The curves in the figure indicate the existence of optimum Peclet numbers that minimize the output variance for each Damköhler number. It can also be seen

that the optimum Peclet number increases as the Damköhler number increases. The optimum Peclet number may be viewed in terms of an optimum reaction rate, as noted in the context of Fig. 3(c). Since the reaction rate increases with Damköhler number, the optimum reaction rate may be realized through a reduction in the resin temperature achieved by an increase in the Peclet number. The optimum Peclet number therefore increases with the Damköhler number in Fig. 4(c). Also evident in Fig. 4(c) is the existence of an optimum Damköhler number for each Peclet number, which minimizes the process output variabilities. In the range of Peclet numbers less than 10^4, and those above 10^8, the variance is minimized for $Da = 8 \times 10^{21}$, while $Da = 8 \times 10^{22}$ is found to be the optimum for $10^4 < Pe < 10^8$. For a chosen resin system, since the Damköhler number is a function of the inlet pressure and the wall temperature, it follows that there are optimum process parameter settings that lead to minimum output variances. It may be noted from that of all the parameter combinations studied in Fig. 4(c), Peclet numbers in the range 10^2–10^6 together with $8 \times 10^{21} \leqslant Da \leqslant 8 \times 10^{22}$ lead to robust processing.

Fig. 4(d) presents the objective function, Z (Eq. (10)), as it varies with the Peclet number for different values of the Damköhler number. The variation of the objective functions with the Peclet number exhibits a trend similar to that shown by the dimensionless fill time in Fig. 4(a). The objective function approaches a minimum value asymptotically for very small Peclet numbers, and increases monotonically to attain an asymptotic upper limit as the Peclet number becomes large. While the objective function, Z, increases continuously with the Peclet number, Damköhler numbers of $Da = 8 \times 10^{21}$ and 8×10^{22} are seen to minimize Z for $Pe < 10^3$ and $Pe > 10^3$, respectively.

Fig. 5(a–d) demonstrate the effects of the adiabatic reaction temperature on the process variabilities. As described earlier, the adiabatic reaction temperature is a measure of the temperature rise potential of the resin due to the exothermic cure reaction. Fig. 5(a) shows plots of the mean dimensionless fill time, τ, against the Peclet number, for different values of the adiabatic

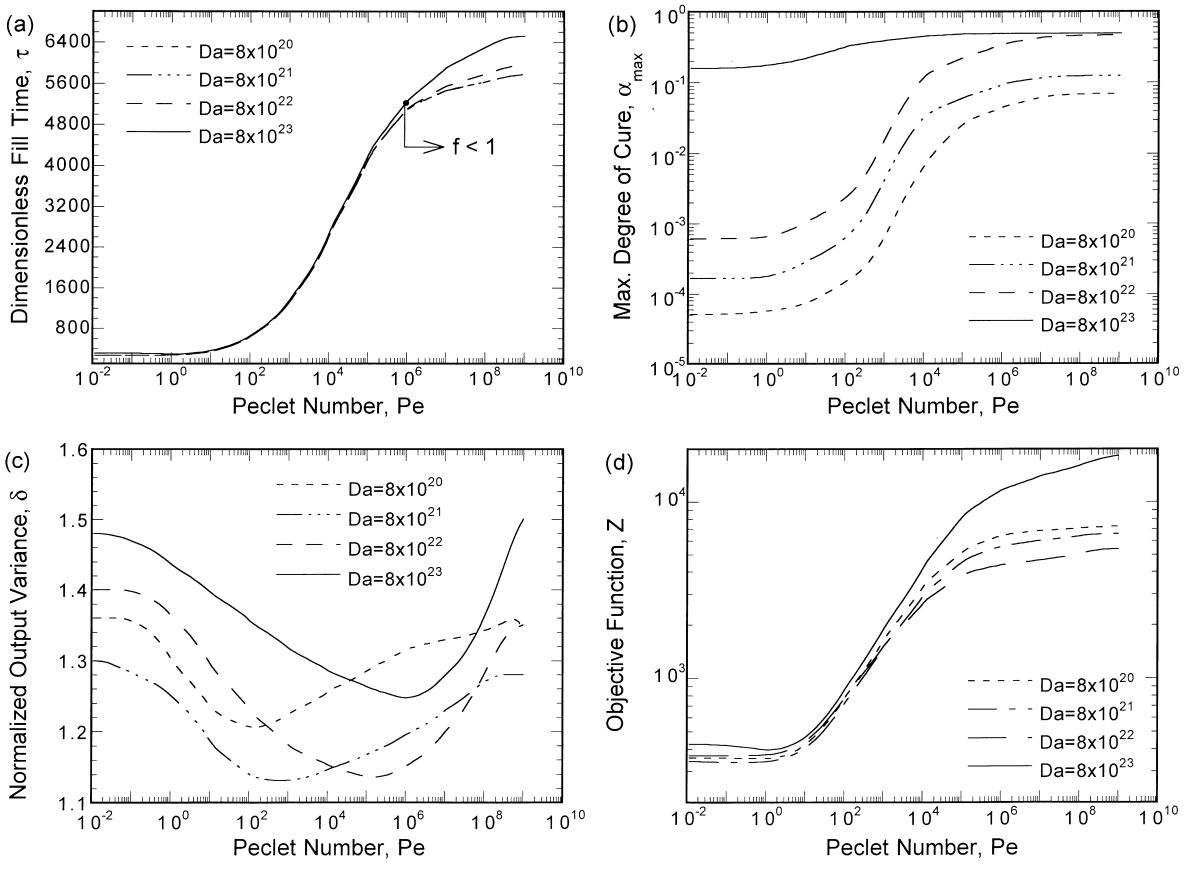

Fig. 4. Variation of the (a) dimensionless fill time, τ, (b) maximum cure at the end of fill, α_{max}, (c) normalized output variance, δ; and (d) multivariate objective function, Z, with Peclet number and Damköhler number, for $\bar{E} = 91.4$, and $\theta_{ad} = 1.0$.

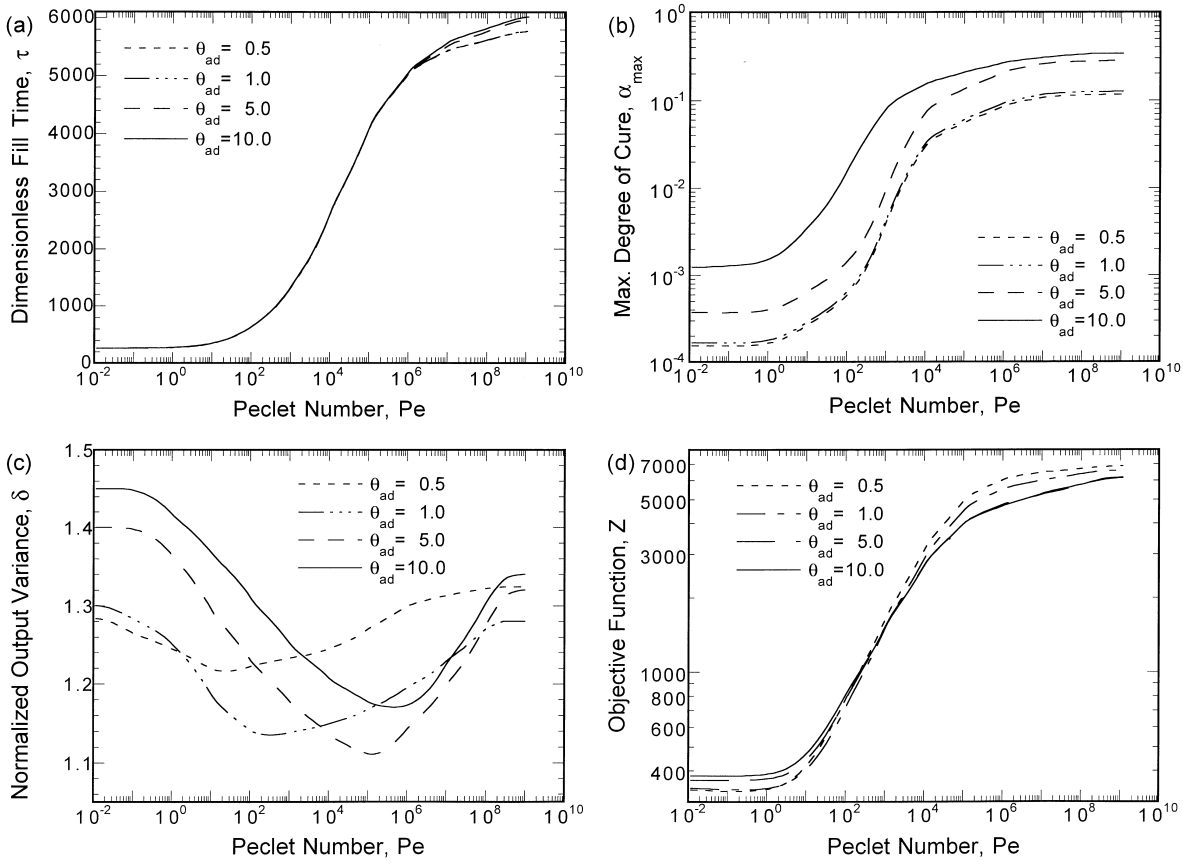

Fig. 5. Variation of the (a) dimensionless fill time, τ, (b) maximum cure at the end of fill, α_{max}, (c) normalized output variance, δ, and (d) multivariate objective function, Z, with Peclet number and the dimensionless adiabatic reaction temperature, for $\bar{E}=91.4$, and $Da=8\times10^{20}$.

reaction temperature, $\theta_{ad}=0.5$, 1.0, 5.0 and 10.0. Fig. 5(b) presents the corresponding mean values of the maximum degree of cure, α_{max}, achieved at the end of mold fill. The variation of the fill time and the maximum degree of cure with the Peclet number remain as noted and explained previously with reference to Figs. 3 and 4. The increased exotherm associated with larger values of the adiabatic reaction temperature results in a greater degree of cure at the end of the filling process, as shown in Fig. 5(b). The extent of crosslinking, however, is seen to be less than 10% for the smaller adiabatic reaction temperatures ($\theta_{ad}=0.5$ and 1.0), which results in a negligible influence on the resin viscosity and the fill time (Fig. 5(a)). For the larger values of the adiabatic reaction temperature ($\theta_{ad}=5.0$ and 10.0), a maximum degree of resin cure of about 30% is attained for the higher Peclet numbers; the corresponding increase on the resin viscosity causes the longer fill times evident in Fig. 5(a). Overall, however, the influence of the adiabatic reaction temperature on the fill time is seen to be minimal, with the maximum variation being about 3% for the higher Peclet numbers. Furthermore, unlike the results of the studies on the variation of the dimensionless activation energy and the Damköhler number (Figs. 3(b) and 4(b)), the degree of cure was found to remain below the gel point, implying a 100% mold fill (equivalently, $f=1$), over the entire range of adiabatic reaction temperatures and Peclet numbers studied.

The cumulative normalized variance on the fill time and the degree of cure are plotted in Fig. 5(c), as a function of the Peclet number and the adiabatic reaction temperature. Analogous to the observations in Fig. 3(c) and 4(c), the variance is seen to be minimized for particular values of the Peclet number. Since the exotherm associated with higher values of the adiabatic reaction temperature tends to enhance the reaction rate, the optimum Peclet number itself increases with the adiabatic reaction temperature, thereby reducing the conduction heat transfer from the mold walls, so as to maintain the reaction rate within an optimum range that minimizes the cumulative variance. The con-

sideration of optimum reaction rate also explains the existence of optimum adiabatic reaction temperature values for fixed Peclet numbers. It is evident from Fig. 5(c) that the optimum θ_{ad} values are as follows: 0.5 for $Pe < 1$; 1.0 for $1 < Pe < 10^4$ and $Pe > 10^8$; and 5.0 for $10^4 < Pe < 10^8$. Fig. 5(c) further reveals that the adiabatic reaction temperatures between 1 and 5 combined with Peclet numbers in the range 10^2–10^6 lead to the smallest variance overall, based on the parametric values investigated. It follows from the definition of the dimensionless adiabatic temperature (Eq. (7)) that values of θ_{ad} on the order of unity signify an isothermal-like mold filling where the heat of the reaction potentially raises the fiber-resin mix temperature to that of the mold wall. It is interesting to note that such a configuration minimizes the output variability for most of the Peclet numbers.

The influence of the adiabatic reaction temperature and the Peclet number on the multi-attribute objective function, Z, is illustrated in Fig. 5(d). The overall variation is dominantly governed by that of the fill time, and the objective function increases monotonically with the Peclet number. In the range of Peclet numbers less than about 10^4, the maximum variation in the objective function value with respect to θ_{ad} is observed to be less than 5%. Nevertheless, the fact that the objective function is minimized by the lower adiabatic temperature values ($\theta_{ad} = 0.5$ and 1.0) in this range of Peclet numbers is noteworthy. On the other hand, in the high Peclet number range ($Pe > 10^4$), the optimum adiabatic reaction temperature shifts to the higher values of 5.0 and 10.0.

The general trend seen from Figs. 3–5 indicates the existence of specific ranges of the dimensionless groups that minimize the normalized output variance, δ, and the multi-attribute objective function, Z. Since the dimensionless groups incorporate both the material parameters and process design variables, the optimum values determined for these nondimensional quantities translate into optimal operating conditions for a given material system, and can be expressed in terms of such parameters as the resin inlet temperature, T_o, the mold wall temperature, T_w, and the inlet pressure, p_i. Alternatively, if material selection and preform design were to be made based on robust processing considerations, the optimum values may be used for a concurrent material and process design.

The combination of the stochastic modeling framework presented in this article, with a numerical optimization technique (such as nonlinear programming) will provide a valuable tool for stochastic process optimization. Since the process simulations for the various samples are independent of one another, use of parallel processing may be explored to improve computational times for stochastic analysis and optimization. Furthermore, comparison of the optimum configurations derived from the stochastic analyses with the experimental results obtained from statistical design of experiments technique [8–10] will offer a fundamental bridge between the experimental and the theoretical approaches. Investigations are presently underway on the foregoing issues, and will be reported in the future.

5. Conclusions

This paper presented a stochastic analysis methodology for investigating the parameter uncertainties associated with nonisothermal mold filling during resin transfer molding processes. The analysis was performed in terms of suitably formulated dimensionless groups, and the process output variabilities were studied as a function of these nondimensional quantities. Based on parametric studies, optimum values of the dimensionless groups that lead to minimum fill times and output variances, while maximizing the degree of cure attained at the end of mold filling, were identified. The optimum values of the dimensionless groups translate into optimum design of material and process parameters in practical processing. Overall, the methodology presented provides a fundamental science-based capability for robust process designs in the face of realistic parametric uncertainties.

Acknowledgements

This research work was funded by the United States Office of Naval Research through a Young Investigator Award (Contract No. N00014-96-1-0726), with Mr James J. Kelly as the Scientific Officer. Their support is gratefully acknowledged. The authors also wish to thank Dr Shortencarier of the Sandia National Laboratories for providing the numerical code for the Latin Hypercube Sampling procedure.

References

[1] S.G. Advani, Flow and rheology in polymer composites manufacturing, in: S.G. Advani (Ed.), Composite Materials Series, vol. 10, Elsevier, New York, 1994.

[2] M.V. Bruschke, S.G. Advani, A numerical simulation of resin transfer mold filling process, ANTEC '89 (1989) 1769–1773.

[3] Y. Chen, C.W. Macosko, H.T. Davis, Wetting of fiber mats for composites manufacturing, AIChE Journal 41 (1995) 2261–2281.

[4] Z. Cai, Simplified mold filling simulation in resin transfer molding, Journal of Composite Materials 26 (1992) 2606–2630.

[5] J.P. Coulter, S.I. Guceri, Resin impregnation during composites manufacturing: theory and experimentation,

Composites Science and Technology 35 (4) (1989) 317–330.

[6] S. Li, R. Gauvin, Numerical analysis of the resin flow in resin transfer molding, Journal of Reinforced Plastics and Composites 10 (1991) 314–327.

[7] L.J. Lee, W.B. Young, R.J. Lin, Mold filling and cure modeling of RTM and SRIM processes, Composite Structures 27 (1994) 109–120.

[8] A.C. Loos, G.S. Springer, Curing of epoxy matrix composites, Journal of Composite Materials 17 (1983) 135–169.

[9] C.D. Han, K.W. Lem, Chemorheology of thermosetting resins. I. The chemorheology and curing kinetics of unsaturated polyester resin, Journal of Applied Polymer Science 28 (1983) 3155–3182.

[10] K.W. Lem, C.D. Han, Chemorheology of thermosetting resins. II. Effect of particulates on the chemorheology and curing kinetics of unsaturated polyester resin, Journal of Applied Polymer Science 28 (1983) 3183–3206.

[11] K.W. Lem, C.D. Han, Chemorheology of thermosetting resins. III. Effect of low-profile additive on the chemorheology and curing kinetics of unsaturated polyester resin, Journal of Applied Polymer Science 28 (1983) 3207–3225.

[12] G. Taguchi, Introduction to Quality Engineering, UNIPUB/Kraus International, New York, 1986.

[13] J.E. Campbell, B.S.R. Rao, An uncertainty analysis methodology applied to sheetpile Cofferdam design, Hydraulic Engineering 41 (1987) 36–41.

[14] G. Apostolakis, The concept of probability in safety assessments of technological systems, Science 250 (1990) 1359–1364.

[15] U.M. Diwekar, E.S. Rubin, Stochastic modeling of chemical processes, Computers and Chemical Engineering 15 (2) (1991) 105–114.

[16] U.M. Diwekar, J.R. Kalagnanam, Efficient sampling technique for optimization under uncertainty, AIChE Journal 43 (2) (1997) 440–447.

[17] S.K. Padmanabhan, R. Pitchumani, Stochastic analysis of the resin transfer modeling process, in: R. Gibson, G.M. Newaz (Eds.), Proceedings of the 12th Conference of the American Society for Composites, Technomic, Lancaster, 1997, pp. 797–806.

[18] S.K. Padmanabhan, R. Pitchumani, Stochastic analysis of isothermal cure of resin systems, Polymer Composites 20 (1) (1999).

[19] R.L. Iman, M.J. Shortencarier, A FORTRAN77 program and user's guide for generation of Latin Hypercube and random samples for use with computer models, Technical report, NUREG/CR-3624, SAND83-2365, Sandia National Laboratories, Albuquerque, 1984.

[20] R. Pitchumani, B. Ramakrishnan, A fractal geometry model for evaluating permeabilities of porous preforms used in liquid composite molding, International Journal of Heat and Mass Transfer 42 (12) (1999) 2219–2232.

[21] S.V. Patankar, Numerical Heat Transfer and Fluid Flow, Hemisphere, Washington D.C., 1980.

[22] H. Niederrieter, Random Number Generation and Quasi-Monte Carlo Methods, Society for Industrial and Applied Mathematics, Philadelphia, 1992.

[23] G. Morgan, M. Henrion, Uncertainty: A Guide to Dealing with Uncertainty in Quantitative Risk and Policy Analysis, Cambridge University Press, New York, 1990.

[24] R.L. Iman, Uncertainty and sensitivity analysis for computer modeling applications, Reliability Technology 28 (1992) 153–168.